Anal. Chem. **2004,** *76,* 2367−2373

Microchip Dialysis of Proteins Using in Situ Photopatterned Nanoporous Polymer Membranes

Simon Song, Anup K. Singh, Timothy J. Shepodd, and Brian J. Kirby*

Sandia National Laboratories, P.O. Box 969, MS 9951, Livermore, California 94551

Chip-level integration of microdialysis membranes is described using a novel method for in situ photopatterning of porous polymer features. Rapid and inexpensive fabrication of nanoporous microdialysis membranes in microchips is achieved using a phase separation polymerization technique with a shaped UV laser beam. By controlling the phase separation process, the molecular weight cutoffs of the membranes can be engineered for different applications. Counterflow dialysis is used to demonstrate extraction of low molecular weight analytes from a sample stream, using two different molecular weight cutoff (MWCO) membranes; the first one with MWCO below 5700 for desalting protein samples, and the second one with a higher MWCO for size-based fractionation of proteins. Modeling based on a simple control volume analysis on the microdialysis system is consistent with measured concentration profiles, indicating both that membrane properties are uniform, well-defined, and reproducible and that diffusion of subcutoff analytes through the membrane is rapid.

In general, real-world biological samples require extensive pretreatment before they can be analyzed in a miniaturized device. These pretreatment steps may include separation or classification of cells, membrane fragments, and other particles from soluble molecular analytes, extraction of a specific molecular weight class of proteins (for example, extraction of cytokines from blood samples and elimination of albumin), or desalting of high-ionic strength protein solutions. In the latter case, desalting is typically required because the high ionic strength reduces the sensitivity and stability of the downstream analytical instrument such as a mass spectrometer or electrophoresis device.

Enormous research efforts in the past decade have been applied to automate biological analyses and to reduce sample consumption and cost. The efforts have led to development of many microfabricated devices performing separation, mixing, reaction, detection, or preconcentration.[1,2] In particular, extraction of analytes from complex samples has been achieved using variations in diffusivity,[3,4] transport between co- or counterflowing immiscible phases,[5] and selective transport through membranes.[6−9]

Dialysis is a proven method for efficient cleanup of macroscale biological samples. It separates sample components based on selective diffusion across a porous membrane, typically made of regenerated cellulose, cellulose acetate, or poly(vinylidene fluoride). The membrane properties allow for separation of smaller components (e.g., salts) from larger components (e.g., proteins). However, macroscale dialysis can require large amounts of sample and is often time-consuming and hard to integrate.

For analysis of minute amounts of samples, various microdialysis systems have been proposed to overcome the limitations of macroscale dialysis. These microdialysis systems can be roughly categorized in three classes based on the dialyzing medium type: sandwiched membrane, dialysis tube, or microdialysis probe. The first type uses a commercial dialysis membrane sandwiched between microfabricated chips and has been used to demonstrate desalting of DNA and protein samples,[6] separation of low molecular weight constituents from an ampholyte mixture,[7] and drug-screening and residue analysis[8] prior to electrospray ionization mass spectroscopy. A dual microdialysis system using two membranes sandwiched between three chips was demonstrated to remove both low and high molecular weight species from a complex biological sample.[9]

Devices in the second category have been employed by surrounding a dialysis tube with a larger buffer tube,[10−12] channel,[13] or reservoir[14] and connecting the output to an analytical instrument through capillaries to perform online microdialysis for a sample cleanup. Sample solutions are injected to the dialysis tube while dialysis buffers are pumped into the gap between the dialysis tube and surrounding medium.

Finally, devices in the last category are fabricated using microdialysis probes. Microdialysis probes are commonly used

* To whom correspondence is to be addressed. Email: bjkirby@sandia.gov.

(1) Reyes, D. R.; Isossifidis, D.; Auroux, P.-A.; Manz, A. *Anal. Chem.* **2002**, *74*, 2623−2636.
(2) Auroux, P.-A.; Isossifidis, D.; Reyes, D. R.; Manz, A. *Anal. Chem.* **2002**, *74*, 2637−2652.
(3) Schilling, E. A.; Kamholz, A. E.; Yager, P. *Anal. Chem.* **2002**, *74*, 798−1804.
(4) Munson, M. S.; Cabrera, C. R.; Yager, P. *Electrophoresis* **2002**, *23*, 2642−2652.
(5) Tokeshi, M.; Minagawa, T.; Uchiyama, K.; Hibara, A.; Sato, H.; Hisamoto, H.; Kitamori, T. *Anal. Chem.* **2002**, *74*, 1565−1571.
(6) Xu, N.; Lin, Y.; Hofstadler S. A.; Matson D.; Call, C. J.; Smith, R. D. *Anal. Chem.* **1998**, *70*, 3553−3556.
(7) Lamoree, M. H.; Van Der Hoeven, R. A. M.; Tjaden, U. R.; Van Der Greef, J. *Mass Spectrom.* **1998**, *33*, 453−460.
(8) Jiang, Y.; Wang, P.-C.; Locascio, L. E.; Lee, C. S. *Anal. Chem.* **2001**, *73*, 2048−2053.
(9) Xiang, F.; Lin, Y.; Wen, J.; Matson, D. W.; Smith, R. D. *Anal. Chem.* **1999**, *71*, 1485−1490.
(10) Benkestock, K.; Edlund, P.-O.; Roeraade, J. *Rapid Commun. Mass Spectrom.* **2002**, *16*, 2054−2059.
(11) Jiang, Y.; Lee, C. S. *J. Mass Spectrom* **2001**, *36*, 664−669.
(12) Liu, C.; Wu, Q.; Harms, A. C.; Simth, R. D. *Anal. Chem.* **1996**, *68*, 3295−3299.
(13) Canarelli, S.; Fisch, I.; Freitag, R. *J. Chromatogr., A* **2002**, *948*, 139−149.
(14) Severs, J. C.; Smith, R. D. *Anal. Chem.* **1997**, *69*, 2154−2158.

10.1021/ac035290r CCC: $27.50
Published on Web 03/05/2004

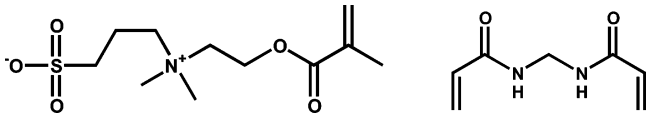

Figure 1. Structures of the monomer 2-(*N*-3-sulfopropyl-*N*,*N*-dimethylammonium) ethyl methacrylate (left) and the cross-linker methylene bisacrylamide (right).

in pharmaceutical and biomedical researches to sample small molecules either in vivo[15−17] or in vitro.[18,19] The probes are typically combined online with an analytical instrument such as a mass spectrometer.

While the aforementioned microdialysis techniques have had success, most of these techniques rely on scale-down of macroscale devices and, hence, suffer from integration issues. We have developed a method for in situ fabrication of dialysis membranes on a microchip to enable programmable chip-level integration of sample processing steps with sample analysis. The ability to photopattern membranes of various sizes, shapes, and molecular weight cutoffs will enable complex sample processing to be integrated at the chip level, allowing facile processing and analysis of small volumes of nascent analytes. Thin (7−50 μm), nanoporous microdialysis membranes are fabricated in situ on glass microchips using phase separation polymerization induced by shaped laser light. This method enables flexible implementation of microdialysis on microchips.

The upcoming sections are organized as follows: first, detailed fabrication techniques and properties of the membranes are described. Second, performance of the microdialysis systems is evaluated through diffusion measurements of various sample analytes along counterflow microdialysis channels. Third, the capability to engineer the pore size of a membrane is demonstrated. Finally, a simple model for describing counterflow dialysis is presented, which facilitates inference of transport properties in the membrane and allows predictions of device performance.

EXPERIMENTAL SECTION

Preparation of Monomer Solution. Unless otherwise specified, all materials are purchased from Sigma-Aldrich (St. Louis, MO). A monomer stock solution is prepared by dissolving 1.00 g of 2-(*N*-3-sulfopropyl-*N*,*N*-dimethylammonium)ethyl methacrylate (SPE) into 1 mL of deionized water containing 33.3 mg of *N*,*N*′-methylenebisacrylamide (BIS). SPE is obtained from Raschig Corp. (Oak Park, IL). The monomer stock solution also contains about 10 ppm Rhodamine 560. Rhodamine 560 enables in situ visualization of the laser profile during laser beam alignment and therefore facilitates precise positioning of the dialysis membrane in the microchip. Monomer stock solutions are replaced every 5 days. Figure 1 shows the structure diagrams of SPE and BIS.

Solvent mixtures are made by combining deionized water and 2-methoxyethanol at varying ratios, as shown in Table 1. The ratio is varied to control the membrane pore size as explained in detail in following sections. Buffer solutions of 10 mM phosphate, pH 6.9, are also prepared from mono- and dibasic potassium phosphate. The monomer stock solution, solvent mixtures, and buffer solutions are mixed in 5:4.7:0.3 ratios by volume. All solutions are sonicated in air for 5 min and filtered with 0.45-μm filters before they are mixed.

Table 1. Monomer Solution Compositions for the Two Membranes Discussed[a]

membrane	monomer stock solution	water	2-methoxy-ethanol	10 mM phosphate buffer, pH 6.9	total
low MWCO	5.0	3.7	1.0	0.3	10.0
high MWCO	5.0	1.2	3.5	0.3	10.0

[a] The numbers indicate relative volumes.

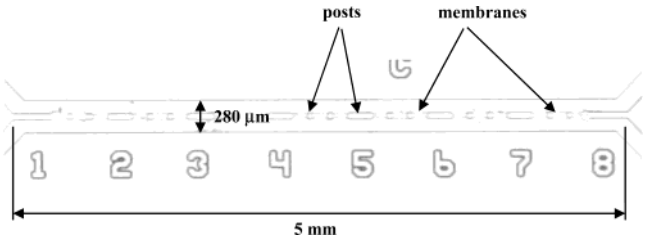

Figure 2. Glass microchannel structure with laser-photopatterned dialysis membrane. The channel depth is 20 μm.

The monomer solution also contains two additives: 0.5% (weight percent of SPE) 2,2′ azobis(2-methylpropanimidamide)-dihydrochloride (V50, Wako Chemicals, Richmond, VA) is present as a photoinitiator, and 150 ppm hydroquinone is present for polymerization inhibition. The use of hydroquinone prevents unwanted polymerization that may occur by heat and molecular diffusion outside the region illuminated by the UV laser beam. V50 was added to the buffer solution and hydroquinone to the deionized water of the solvent mixture.

Microchip. Fused-silica (Corning 7980) microchips, fabricated in-house, are used in the present studies. Standard photoresist, UV patterning, and isotropic HF wet-etch steps as specified in ref 20 are used for fabrication with the following differences: (a) substrates are 750-μm Corning 7980 fused-silica wafers (Sensor Prep Services, Inc., Elburn, IL) with 150-nm amorphous LPCVD-desposited silicon hard mask; (b) patterning is achieved with SJR 5740 photoresist and Microposit developer (Shipley Corp., Marlborough, MA); (c) silicon is etched with an oxygen ash and SF_6 plasma treatment; (d) silica is etched with 49% HF at 1.2 μm/min; and (e) thermal diffusion bonding occurs at 1150 °C. As shown in Figure 2, the channel length of the microdialysis system is 5 mm, the total width 280 μm, and the depth nominally 20 μm. The membrane thickness is nominally 35 μm. The channel has both an inlet and an outlet at each end. Silica supporting posts along the channel centerline facilitate rapid fabrication of membranes and maximize pressure holdoff of the membrane. The posts (consisting of unetched silica) span the entire depth of the channel and are of 50-μm diameter to ensure thermal diffusion bonding with the cover wafer.

(15) Deterding, L. J.; Dix, K.; Burka, L. T.; Tomer, K. B. *Anal. Chem.* **1992**, *64*, 2636−2641.
(16) Lin, S.; Slopis, J. M.; Butler, I. J.; Caprioli, R. M. *J. Neurosci. Methods* **1995**, *62*, 199−205.
(17) Fuh, M.-R.; Tai, Y. L.; Pan, W. H. T. *J. Chromatogr., B* **2001**, *752*, 107−114.
(18) Kobayashi, N.; Fujimori, I.; Watanabe, M.; Ikeda, T. *Anal. Biochem.* **2000**, *287*, 272−278.
(19) Kerns, E. H.; Volk, K. J.; Klohr, S. E.; Lee, M. S. *J. Pharm. Biomed. Anal.* **1999**, *20*, 115−128.
(20) Throckmorton, D. J.; Shepodd, T. J.; Singh, A. K. *Anal. Chem.* **2002**, *74*, 784−789.

To facilitate covalent attachment of the membrane to the silica surface, the silica surface is coated with 3-(trimethoxysilyl)propyl acrylate through acid-catalyzed hydrolysis of the methoxy groups followed by condensation with the surface silanols. Channels are first conditioned by 30-min flushes with 1 M HCl and then 1 M NaOH, then rinsed with deionized water, and dried. The microchannels are incubated for 30 min with a solution consisting of a 2:2:1 (vol) mixture of deionized water, glacial acetic acid, and 3-(trimethoxysilyl)propyl acrylate. The channel is then rinsed thoroughly with deionized water and 1-propanol.

Detection Instruments. Properties and performance of the microdialysis membranes were evaluated by measuring diffusion of various analytes in microdialysis systems. A variety of labeled proteins and one dye (used as an analogue for salts or other low molecular weight analytes) were used to provide a relatively broad molecular weight spectrum: 10 ppm Rhodamine 560 in water, 0.5 mg/mL FITC-insulin in a pH 9.0, 50 mM borate buffer; 0.1 mg/mL FITC-lactalbumin in a pH 8.4, 50 mM borate buffer; 0.8 mg/mL FITC-bovine serum albumin in a pH 7.1, 10 mM phosphate buffer; and 0.5 mg/mL FITC-antibiotin in a pH 6.8, 10 mM phosphate buffer.

The concentration of the dye or proteins in the dialysis channels was calculated by measuring fluorescence signals with a microscope and camera system (Olympus, model IX70). The maximum concentration of the proteins and dye was kept low enough to prevent self-quenching of the fluorescence and saturation of the camera CCD, so the fluorescence signal could be assumed proportional to the concentration. Between the measurements, the channels were thoroughly rinsed with water, isotonic phosphate-buffered saline, and acetonitrile.

RESULTS

Two microdialysis membranes with thicknesses near 35 μm were fabricated inside 5-mm-long fused-silica microchannels. Each membrane was engineered to have a specific pore size distribution and therefore molecular weight cutoff (MWCO). In the following paragraphs, the detailed fabrication method and general characteristics of the two sets of membranes are described. Then, the performance of the two systems with different MWCOs and techniques for controlling the MWCO of the membranes are discussed.

Formation and Characteristics of Microdialysis Membranes. In situ polymerization of membranes is achieved by filling the microchannels with a monomer solution and then initiating polymerization and phase separation with the focused output of a UV laser. The microchannel is filled with the solution through capillary action, the application of vacuum, or both. After filling, the four ports of the microchannel are covered to minimize evaporation. The fluid in the channel is allowed to come to a quiescent state for 30 min under ambient light. Allowing the flow to decay is crucial for optimum resolution, since any pressure-induced fluid motion due to hydrostatic head or surface tension will adversely affect the resolution of the photopatterning.

Dialysis membranes are fabricated piecewise through local exposure to shaped laser light. The 355-nm beam of a 10-kHz, passively Q-switched, frequency-tripled Nd:YAG laser (JDS Uniphase, model NV-10210-100) is spatially filtered with a slit (Melles Griot, model 07SLT001/S) and focused with a series of spherical and cylindrical lenses into a sheet of approximate thickness 4−30 μm (Figure 3). Because the profile of the beam is Gaussian, the illumination is not perfectly uniform; however, the beam irradiance is uniform to within 20% along the slit image axis and to within 5% normal to that axis. Local excitation of the photoinitiator in the solution generates free radicals leading to chain polymerization. This results in phase separation in the irradiated region as the polymerization proceeds. The time of each polymerization step varies depending on the formula of monomer solution used, ranging from 1 to 4 min, approximately, and total fabrication time in the current configuration (including all fabrication steps) is ~3 h. The membrane was fabricated in ~600-μm pieces, corresponding approximately to the length of the laser sheet. The channel was flushed and filled with a fresh monomer solution between each laser exposure.

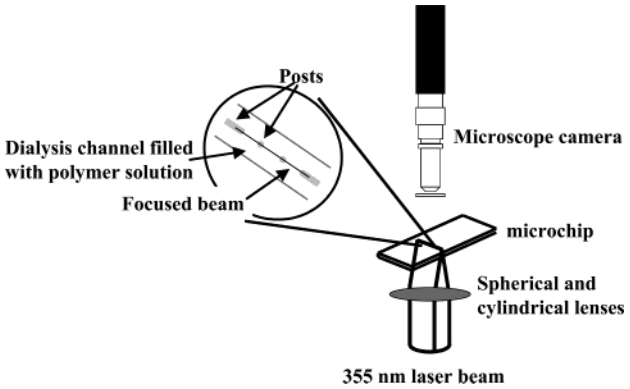

Figure 3. Schematic of optical setup for in situ phase separation polymerization (not to scale).

The aforementioned projection lithography technique was developed to enable fabrication of thin (7−50 μm) polymer membranes within microchannels. While contact lithography is straightforward and provides excellent resolution when the mask can be brought directly into contact with the exposed surface, patterning of small features within the microchannels of fused-silica microchips is limited by diffraction through the chip substrate. For larger (>100 μm) feature size, contact lithography has been successfully implemented for patterning polymer features.[20−22] However, for the chips used in this study (1-mm wafer thickness), uniform illumination of features below 60 μm in size is impossible with contact lithographic techniques, and the desired membrane thicknesses are well below this value. By controlling the feature size with far-field rather than near-field optics, limitations based on wafer thickness can be eliminated.

The microdialysis membranes presented here maintain their properties upon exposure to a wide range of pH, polar solvents, and protein analytes and have performed well upon repeated use. The microdialysis systems have been used tens of times for measurements since fabrication. Also, the channel and membranes have been rinsed with 380 mM NaCl solution, water, and acetonitrile numerous times without a change in performance. The membranes withstand a pH range varying at least from 2.7 to 9.0. No distinguishable proteins stuck to the membranes after the channels were rinsed with water and a 380 mM NaCl solution, consistent with the hydrophilic nature of the zwitterionic polymer.

(21) Beebe, D. J.; Moore, J. S.; Yu, Q.; Liu, R. H.; Kraft, M. L.; Jo, B. H.; Devadoss, C. *Proc. Natl. Acad. Sci. U.S.A.* **2000**, *97*, 13488−13493.
(22) Yu, C.; Davey, M. H.; Svec, F.; Frechet, M. J. *Anal. Chem.* **2001**, *73*, 5088−5096.

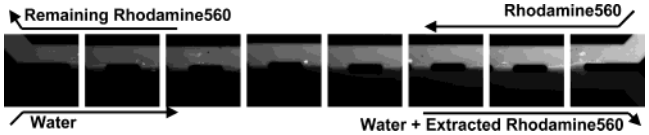

Figure 4. Rhodamine 560 extraction in a counterflow dialysis configuration with the low MWCO membrane. The distance between the centers of the first and last images is 4.8 mm.

The posts in the microchannel maximize the mechanical strength of the membranes so that the membranes can withstand a pressure drop of ~1 bar. Vacuum pressure could be used to manipulate fluids as part of the fabrication process or for analysis. As needed, higher pressure holdoff can be achieved by changing the polymer formulation to increase the degree of cross-linking. However, this will also affect pore size and MWCO and was not explored in this work.

Low MWCO Microdialysis System. A counterflow microdialysis system with MWCO below 5700 was fabricated in a 5-mm-long microchannel by patterning membranes in the middle of the microchannel to separate the sample (top) and perfusion (bottom) flows. A solvent mixture consisting of a 3.7:1.0 ratio of deionized water and 2-methoxyethanol was used; the overall composition of the monomer solution is shown in Table 1. A picture of the membranes is shown in Figure 2. The membrane thickness was measured as 35 ± 4 μm. The variations exist due to the slight intensity decrease in the wings of the laser profile.

Images of the sample analyte concentration in counterflow configuration were used to evaluate the performance of the microdialysis system and the MWCO of the membranes. Figure 4 shows images of the microdialysis channels at steady state using Rhodamine 560 as a sample analyte. The right end of the upper channel (sample channel) was connected to a reservoir filled with 20 μL of the Rhodamine 560 solution. The left end of the lower channel (perfusion channel) was connected to a reservoir with 100 μL of water. The other two ends of the channel were open to the air. Thus, the flows were driven by the hydraulic head difference between the reservoir and open port. The channels were in a counterflow configuration; i.e., the sample liquid flowed right to left and the perfusion liquid left to right. It is clear from Figure 4 that the Rhodamine 560 concentration in the sample channel decreases along the flow. For the same experiment, Figure 5 shows steady-state profiles of the Rhodamine 560 concentration variation in the sample and perfusion channels. The concentration is averaged across each channel, and then normalized by the value at the inlet of the sample channel. The dye concentration in the sample channel was reduced by 58% over the 5-mm length while the perfusion channel has a 17% increased dye concentration at the exit. The increase in concentration in the perfusion stream is smaller and more difficult to see from the gray scale image in Figure 4 but is quite apparent in Figure 5. The average flow rate in the sample channel was estimated as 10 nL/min by tracking particle streaks exposed in flow images. The average flow in the perfusion channel was estimated to be 35 nL/min.

Diffusion of dye and various labeled peptides/proteins including insulin (5700), lactalbumin (14 000), bovine serum albumin (66 000), and anti-biotin (150 000) through the membrane was observed in order to estimate its MWCO. Figure 6 shows images of the microdialysis channel with the insulin solution, which are

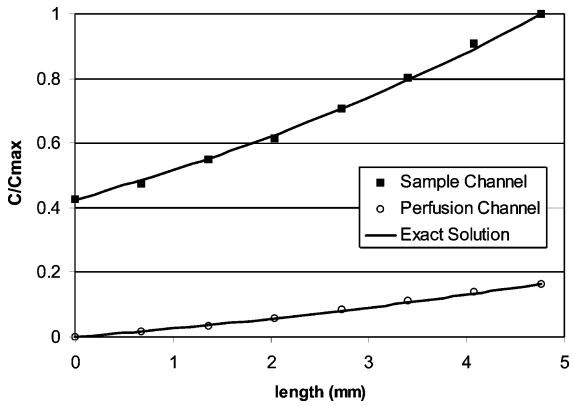

Figure 5. Concentration variations of Rhodamine 560 in the sample and perfusion channels for the low MWCO membrane. The exact solutions were obtained for $\alpha = 1.0$ and $\beta = 3.5$. The difference in the spatial concentration gradients in the two channels is caused by differing flow rates.

Figure 6. Lack of extraction of FITC-insulin (5700) in a counterflow dialysis configuration using the low MWCO membrane. The distance between the centers of the first and last images is 4.8 mm.

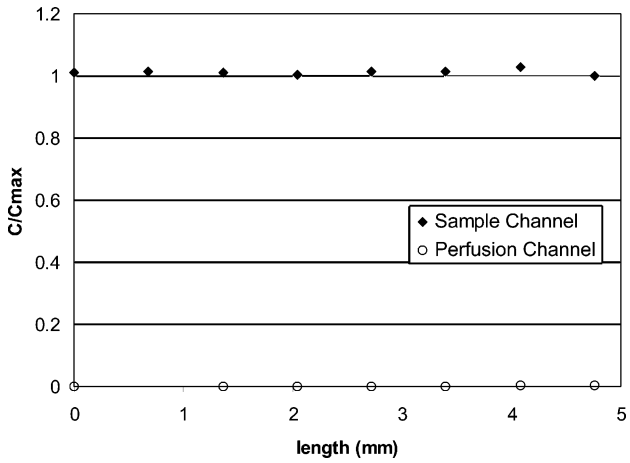

Figure 7. Concentration variations of FITC-insulin in the sample and perfusion channel for the low MWCO membrane. In this case, $k = \alpha = 0$.

representative of the results achieved for all analytes with molecular weight of >5000. No distinguishable concentration decrease along the channel was observed, as can be seen quantitatively in Figure 7. The present membrane thus has a MWCO below 5700, indicating that this membrane could be effective for desalting protein solutions for mass spectroscopy or electrokinetic analysis or could be used to extract low MW analytes such as amino acids, hormones, or neurotransmitters from complex samples for analysis.

High MWCO Microdialysis System. A high MWCO microdialysis system was fabricated using similar techniques but a different polymerization solvent. The relative amount of deionized water (a good solvent for the polymer) versus 2-methoxyethanol (a poor solvent) was varied to modify the thermodynamics of phase separation and thus the pore size. High MWCO membranes

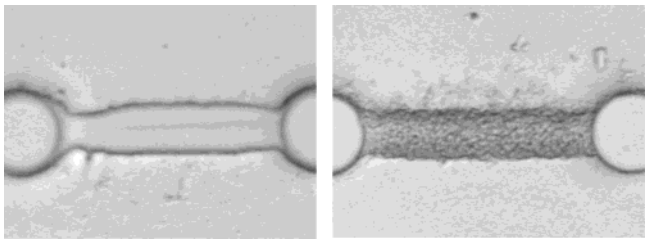

Figure 8. Left: low MWCO membrane (deionized water:2-methoxyethanol = 3.7:1). Right: high MWCO membrane (deionized water: 2-methoxyethanol = 0.34:1). The post diameter is ~50 μm.

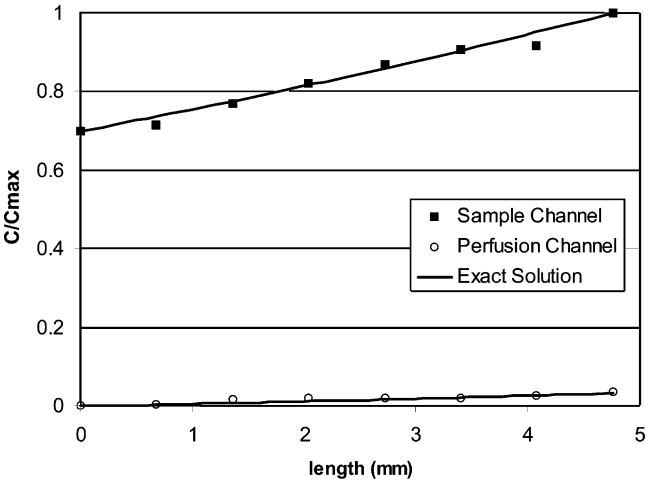

Figure 9. FITC-lactalbumin extraction by counterflow dialysis using the high MWCO membrane. The exact solutions were obtained for $\alpha = 0.38$ and $\beta = 10$. The difference in the concentration gradients in the two channels is caused by differing flow rates.

were fabricated in a 5-mm-long microchannel by using a solvent mixture with a 1.2:3.5 ratio of deionized water and 2-methoxyethanol, as shown in Table 1. The overall ratio of monomer stock solution, solvent mixture, and buffer solution and the concentration of the additives remained the same in both cases. Figure 8 shows a visual comparison of the low MWCO membrane shown in Figure 2 to a high MWCO membrane. The channels were filled with water, and the images were taken in transmission with a light microscope and camera. Large structures of pores are observed in the high MWCO membrane while the pores in the low MWCO membrane are so small that the membrane is semitransparent.

Measurements of diffusional transfer in the high MWCO system provide strong evidence that the pore size of the microdialysis membranes can be controlled by varying the ratio of the solvent mixture. A sample analyte (lactalbumin) was introduced to the sample channel with the high MWCO membranes in the same way as described earlier. Figure 9 shows the concentration profiles in the sample and perfusion channels. Unlike the low MWCO membranes, these membranes allow diffusion of lactalbumin. As a result, the concentration drops by 30% in the sample channel. In a similar configuration, 80% extraction of Rhodamine 560 was achieved using the more porous high MWCO microdialysis system.

DISCUSSION

Simple one-dimensional analysis of the counterflow microdialysis system facilitates identification of key membrane characteristics and extrapolation from the current design to other

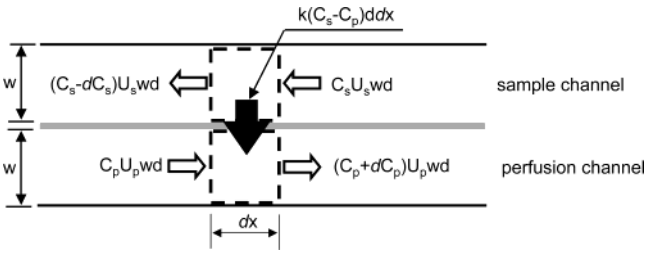

Figure 10. Concentration fluxes for control volumes in microdialysis channels. The concentration on either side of the membrane is assumed uniform: *C*, concentration normalized by the value at the sample channel inlet; *U*, flow speed; *w*, channel width; *d*, channel depth; *k*, mass-transfer coefficient; *x*, distance from the perfusion channel inlet. The total length of the channel is *L*, and subscripts s and p indicate the sample and perfusion channels, respectively.

systems with different dimensions or shapes. The transfer in a counterflow microdialysis system can be simplified by treating the concentrations on either side of the membrane as uniform. This is equivalent to averaging the concentration across channels, as was done to produce Figure 5 and Figure 9. This assumption is suitable at low Peclet number, but tends to underestimate the membrane diffusivity at high Peclet number; thus, this assumption is useful for generating a simple intuitive model but cannot be applied quantitatively in all cases, as will be seen in the paragraphs to follow. For this simplified case, control volumes can be drawn around the sample or perfusion liquids, and the concentration evolution equations consist of convective fluxes parallel to the membrane and diffusive fluxes through the membrane (Figure 10). At steady state, the fluxes sum to zero, leading to one-dimensional differential equations for the distribution of concentration in the sample and perfusion liquids:

$$\frac{dC_s}{dx} = (C_s - C_p)\frac{k}{U_s w} \tag{1}$$

$$\frac{dC_p}{dx} = (C_s - C_p)\frac{k}{U_p w} \tag{2}$$

with notation defined in Figure 10. Here k is an overall (area-averaged) mass-transfer coefficient that takes into account both polymer membrane and silica support post. Integration of the two equations with normalized boundary conditions that $C_s(x=L) = 1$ and $C_p(x=0) = 0$ yields exact solutions for concentration variation along the sample and perfusion channels as follows.

$$C_s = \frac{\beta \exp\left\{\alpha\frac{(\beta-1)}{\beta}\frac{x}{L}\right\} - 1}{\beta \exp\left\{\alpha\frac{(\beta-1)}{\beta}\right\} - 1}; \quad \beta \neq 1 \tag{3}$$

$$C_p = \frac{\exp\left\{\alpha\frac{(\beta-1)}{\beta}\frac{x}{L}\right\} - 1}{\beta \exp\left\{\alpha\frac{(\beta-1)}{\beta}\right\} - 1}; \quad \beta \neq 1 \tag{4}$$

Here $\alpha \equiv kL/U_s w$, and $\beta \equiv U_p/U_s$. α and β are two key nondimensional parameters that determine performance of the

microdialysis system. α is the ratio of transverse to longitudinal mass-transfer rates in the sample channel, indicating how efficiently the system can extract analytes. β is the velocity ratio of the two channels and indicates how extensively the concentration in the perfusion liquid is perturbed by the system.

The solutions for limiting cases such as $\beta \rightarrow 1$ or $\beta \rightarrow \infty$ provide useful insight in understanding characteristics of the counterflow mass-transfer system. For $\beta \rightarrow 1$ ($U_p = U_s$), eqs 3 and 4 become as follows.

$$C_s = \frac{\alpha x/L + 1}{\alpha + 1} \tag{5}$$

$$C_p = \frac{\alpha x/L}{\alpha + 1} \tag{6}$$

implying that $dC_s/dx = dC_p/dx = \alpha/[(\alpha + 1)L]$. This means that the concentration difference of both the channels remains the same and that the ratio of exit concentrations at the perfusion and sample channels is equal to α. For $\beta \rightarrow \infty$ ($U_p \gg U_s$), eqs 3 and 4 become as follows.

$$C_s = \exp\left\{\alpha\left(\frac{x}{L} - 1\right)\right\} \tag{7}$$

$$C_p = 0 \tag{8}$$

Thus, the concentration at the sample channel exit ($x = 0$) is equal to $1/e^{\alpha}$, meaning that 63% of the analytes are transferred to the perfusion channel when $\alpha = 1$.

Concentration profiles in Figures 5 and 9 can be used to infer the analyte-specific mass-transfer coefficients (k) of the membranes, which allow idealized performance for this system to be estimated. For each concentration profile, α and β are chosen by a regression analysis to optimally fit the measured data. α then defines k through the known L, U_p, and w. For example, the data in Figure 5 are fit with values $\alpha = 1.0$ and $\beta = 3.5$. Uniform analyte distribution across each of the sample channel and perfusion channels can be assumed here in the estimation of the overall mass-transfer coefficient since the Peclet number ($U_s w/D$) is low (∼50) for Rhodamine 560 and observed spatial variations normal to the membrane were small. The overall mass-transfer coefficient of the system with the low MWCO membranes is estimated as 1.66 μm/s for Rhodamine 560. The *overall* mass-transfer coefficient is a spatially averaged value that incorporates both the glass posts (for which there is no transfer) and the membrane. Since the membrane area is ∼53% of the total area along the centerline, the *membrane* mass-transfer coefficient is 3.13 μm/s. From this, the diffusivity of Rhodamine 560 within the membrane can be estimated from

$$D_{membrane} = k_{membrane}\delta \tag{9}$$

where δ is the membrane thickness. For the low MWCO membrane, the Rhodamine 560 diffusivity in the membrane is calculated as 110 $\mu m^2/s$, which is ∼31% of the value in water.

Similar calculations can be made on transport through the high MWCO membrane, showing both the general ability of eqs 1 and 2 to describe concentration profiles in the dialysis system and also the limitations caused by the assumption of uniform concentration profiles. The experimental data match well to the exact solutions with $\alpha = 0.38$ and $\beta = 10$ as shown in Figure 9. This leads to the overall mass-transfer coefficient of the system of 0.7 μm/s. However, the Peclet number for the lactalbumin experiment is high (∼200). Thus, the assumption of uniform concentration across a channel results in an underestimation of the membrane mass-transfer coefficient, since the actual concentration drop across the membrane is less than that in the case of the uniform concentration assumption. Correcting for this (∼30%) error by visualizing the complete concentration profile in detail, the *overall* mass-transfer coefficient for lactalbumin is estimated to be 0.9 μm/s and the *membrane* mass-transfer coefficient is estimated to be 1.9 μm/s. The inferred in-membrane diffusivity for lactalbumin in the high MWCO membrane is 67 $\mu m^2/s$, which is 63% of the value in water.

Equation 7 can be used to straightforwardly evaluate the performance of these dialysis systems and quantify expected performance as input parameters (membrane thickness, menbrane length, flow rate, analyte diffusivity) are changed. In particular, since α is the only parameter in eq 7, the system changes that need to be implemented for a specified extraction level are clear. For example, for Rhodamine 560 extraction at the membrane length and sample flow rate shown here, $\alpha = 1$ and ∼60% of the Rhodamine is extracted. A 98% extraction, for example, would require $\alpha = 4$; this could be achieved with a 4-fold increase in channel length (2 mm) or a 4-fold decrease in membrane thickness (9 μm). Extraction of salts and buffer ions, which diffuse more readily than Rhodamine 560, would be even easier to achieve. Since both longer (1 mm) and thinner (7 μm) membranes have been fabricated in our laboratory using these techniques, the path to microchip extraction devices that remove ∼98% of low MW analytes is clear.

The good agreement between the measurements and the exact solutions is indicative of a spatially uniform membrane-transfer coefficient and supports the hypothesis that the membrane properties and pore size distributions are uniform despite piecewise construction. With known mass-transfer coefficients, it is straightforward to use eqs 3 and 4 (or other classical techniques such as log-mean concentration differences or ϵ-NTU analysis) to design microdialysis systems and experiments to generate whatever degree of extraction is required for the intended application.

CONCLUSIONS

Microchip dialysis has been performed on protein samples using integrated dialysis membranes in fused-silica microchips. A novel method for rapid and inexpensive in situ fabrication of microchip dialysis membranes was demonstrated. Nanoporous microdialysis membranes were fabricated in a 5-mm-long microchannel using a phase separation polymerization technique with a shaped laser beam.

A microdialysis system designed for desalting protein samples was designed by using a high water/2-methoxyethanol ratio in the polymerization solvent, leading to small pores. This system allowed diffusion of Rhodamine 560 at ∼31% of the bulk diffusivity in water. As a result, the dye concentration is reduced by 58% in the 5-mm-long sample channel. Monomeric insulin and larger analytes do not diffuse through the membranes, and the molecular

weight cutoff of the present membranes is below 5700. By varying the solvent composition in the monomer/solvent mixture (water and 2-methoxyethanol), the pore size of membranes can be changed to allow diffusion of larger analytes. A higher MWCO microdialysis system was fabricated using a low water/2-methoxyethanol ratio. This system was more porous, allowed faster diffusion of Rhodamine 560, and allowed diffusion of lactalbumin.

The membranes withstand a pressure drop of 1 bar and a pH at least from 2.7 to 9. Protein adhesion to the membrane is minimal. The membranes are readily reproducible without any significant observable property change as evidenced by the good agreement between the measurements and the exact solutions of concentration variation in microdialysis system.

In future work, we plan to incorporate these membranes into integrated systems to allow processing and analysis of cell lysates and serum.

ACKNOWLEDGMENT

The authors thank D.J. Throckmorton and S.A. Pizarro for assistance with fluorescent labeling of proteins, as well as B.W. Wiedenman, S.L. Jamison, W.H. Kleist, and G.B. Sartor for assistance with various aspects of glass wafer microfabrication. This work was supported by the Laboratory Directed Research and Development program at Sandia National Laboratories. Sandia National Laboratories is a multiprogram laboratory operated by Sandia Corp., a Lockheed Martin Co., for the United States Department of Energy under Contract DE-AC04-94AL85000.

Received for review October 31, 2003. Accepted February 5, 2004.

AC035290R